

Evolution of nonlinear waves in compressing plasma

P. F. Schmit, I. Y. Dodin, and N. J. Fisch

Department of Astrophysical Sciences, Princeton University, Princeton, New Jersey 08544, USA

(Received 8 February 2011; accepted 15 March 2011; published online 27 April 2011)

Through particle-in-cell simulations, the evolution of nonlinear plasma waves is examined in one-dimensional collisionless plasma undergoing mechanical compression. Unlike linear waves, whose wavelength decreases proportionally to the system length $L(t)$, nonlinear waves, such as solitary electron holes, conserve their characteristic size Δ during slow compression. This leads to a substantially stronger adiabatic amplification as well as rapid collisionless damping when L approaches Δ . On the other hand, cessation of compression halts the wave evolution, yielding a stable mode. © 2011 American Institute of Physics. [doi:10.1063/1.3574343]

I. INTRODUCTION

Compressing and expanding plasmas can be found throughout nature and the laboratory. In particular, a variety of experimental techniques to compress plasma to thermonuclear temperatures and densities have been explored in the field of inertial confinement fusion.^{1–3} With an eye toward those and similar applications, it was suggested recently that embedding waves in collisionless plasma could yield new tools for manipulating the medium. Specifically, waves might be amplified through compression⁴ and then damp resonantly on a particular species in a switchlike manner at a predetermined moment.⁵ It was also suggested that concentrating energy in a compressing plasma in the form of waves can increase the plasma effective compressibility,⁶ and recent work⁷ has even described the basic thermodynamic cycles whereby the interplay between plasma wave energy and thermal energy could be utilized to construct a plasma heat pump and heat engine. Yet, these studies were focused primarily on linear waves, whereas practical applications may require higher wave amplitudes. Thus, nonlinear effects also need to be explored.

The purpose of this paper is to study such nonlinear effects for wave evolution in one-dimensional (1D) collisionless plasmas undergoing compression, within a paradigmatic model^{5,6} of a bounded system with moving walls. Specifically, addressed here is the evolution of electrostatic Bernstein–Greene–Kruskal (BGK) modes,⁸ which are produced as saturated states of a bump-on-tail instability, like in unbounded plasmas.^{9–14} Unlike linear waves, whose wavelength decreases proportionally to the system length $L(t)$,⁵ we observe that nonlinear waves, such as solitary electron holes,¹⁵ conserve their characteristic size Δ during slow compression. This leads to a substantially higher adiabatic amplification as well as rapid collisionless damping when L approaches Δ . On the other hand, cessation of compression halts the wave evolution, yielding a stable mode. These effects are demonstrated numerically via particle-in-cell (PIC) simulations.

The paper is organized as follows. Section II describes the formation of nonlinear waves produced by the bump-on-tail instability and relates them to those found in unbounded plasma. Section III describes the amplification and subse-

quent collisionless damping of nonlinear waves through compression. In Sec. IV, possible applications of these effects are discussed. Section V summarizes the main results of this paper.

II. FORMATION OF A NONLINEAR WAVE

Saturation of the bump-on-tail instability yields BGK-like modes, which represent quasistatic depressions of the electron density in a self-consistent electric potential. However, in contrast to unbounded plasma, where such modes remain stationary, PIC simulations reveal that they continue to evolve in bounded plasma.

The evolution of electron holes was modeled here using an electrostatic 1D PIC code. The code models the dynamics of electrons bounded by perfectly reflecting walls, at $x=0$ and at $x=L(t)$, such that $\dot{L} = V \leq 0$. To maintain quasineutrality, ions are modeled as an instantaneously charge-neutralizing background. (Simulating the self-consistent ion motion has shown that the results are qualitatively unchanged for an appropriate choice of initial parameters.⁵) To produce a bump-on-tail instability, electrons are initialized randomly in a homogeneous Maxwellian distribution, $f_{M1}(v)$, superposed with smaller, homogeneous, symmetric shifted-Maxwellian bumps, $f_{M2}(v)$ [Fig. 1(a)]. The total initial distribution function $f_0(v)$ is then

$$f_0(v) = n_0 \{ (1 - 2\xi) f_{M1}(v) + \xi [f_{M2}(v + \Delta_v) + f_{M2}(v - \Delta_v)] \}, \quad (1)$$

where $f_{Mj}(v) = \exp(-v^2/2v_{Tj}^2)/\sqrt{2\pi}v_{Tj}$ for $j = 1, 2$. Specifically, the following parameters are taken: the bulk number density n_0 corresponds to the plasma frequency $\omega_p = 10^{11} \text{ s}^{-1}$; the thermal velocities are $v_{T1} = 10^9 \text{ cm/s}$ and $v_{T2} = 0.75v_{T1}$; the beam central speeds are $\Delta_v = 5v_{T1}$; the normalized density of the bumps is $\xi = 0.15$; and, finally, the characteristic initial transit period of BGK modes is given by $T_{tr} \sim L_0/\Delta_v = 4 \times 10^{-10} \text{ s} \approx 6.4\tau_p$, where L_0 is the initial system length and $\tau_p = 2\pi/\omega_p$.

Figure 1 depicts the evolution of the electron phase space density during a strong, initially isotropic bump-on-tail instability in a bounded system without compression. It is seen that electron holes form and then merge such that eventually only

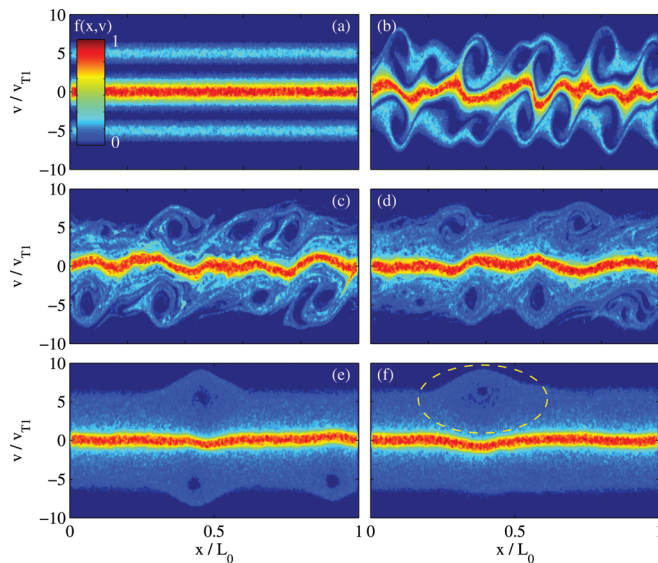


FIG. 1. (Color online) Snapshots of the electron phase space density $f(x, v)$ (in arbitrary units) in bounded plasma without compression. These snapshots show the development of the bump-on-tail instability and subsequent evolution of nonlinear BGK-like modes: (a) $t=0$, initial bump-on-tail distribution; (b)–(e) formation and merging of electron holes; (f) $t=280\tau_p$, final state, corresponding to a solitary electron hole (circled). Time is measured in units $\tau_p = 2\pi/\omega_p$. For specific parameters, see the main text.

one hole survives [Fig. 1(f)]. During the merging, the wave energy is gradually transferred from the wave to electrons (Fig. 2). This effect exists also in unbounded plasma;^{9–11,16} however, the difference here is that slow decay of the wave persists also after the last hole has been formed.

Consider, in particular, the evolution after $t = 500 \tau_p$. In unbounded plasma, this would have been enough time for a

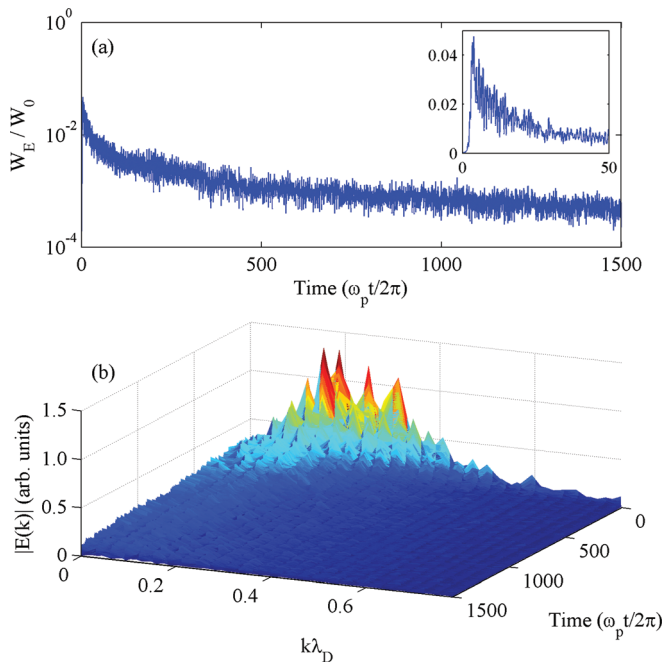


FIG. 2. (Color online) Electric field evolution in bounded plasma without compression. (a) Semilogarithmic plot of the total electrostatic energy W_E normalized to the total plasma energy W_0 . Inset shows a close-up of the first 50 plasma cycles. (b) The absolute value of the electric field spatial Fourier spectrum $E(k)$ vs time t and wavenumber k , measured, correspondingly, in plasma periods $2\pi/\omega_p$ and inverse Debye lengths, λ_D^{-1} .

solitary electron hole to phase-mix and thus yield an equilibrium state. However, for the bounded plasma simulated here, one can observe the wave energy to continue decreasing over the next $1000\tau_p$. This effect is likely due to the interaction between counterpropagating modes; those cause phase-dependent perturbations in the mode structure and thereby lead to further trapping, untrapping, and phase-mixing. Since even a single isolated electron hole produces a counterpropagating hole when it reflects off a wall, there always remains room for more phase-mixing. Hence, collisionless dissipation is never suppressed completely.

This slow damping mechanism provides a caveat to the claim in Ref. 14 that the *time-asymptotic* state of the symmetric bump-on-tail instability is two counterpropagating BGK modes. It also provides a practical example of the limits of the nonlinear superposition principle derived in Ref. 17, which states that only at small enough amplitude can two BGK modes traveling at sufficiently different phase velocities form a plasma equilibrium state. A similar effect was observed in colliding *driven* BGK modes,¹⁸ where the fast interaction of two counterpropagating electron holes resulted in some degradation of their structure.

An example of electron detrapping is shown in Fig. 3. The particle starts off deeply trapped at the bottom of the nonlinear wave potential, which emerged at $t \approx 365\tau_p$. For several hundred plasma periods afterward, Fig. 3(a) shows that the amplitude of the electron bounce oscillations grows, indicating that the particle is transitioning to more weakly trapped orbits closer to the separatrix. Finally, at $t \approx 700\tau_p$, the particle escapes the potential well and becomes untrapped. Since plasma is not being compressed in this simulation, implying the conservation of the total system energy, the energy for detrapping is apparently extracted from modes counterpropagating to that holding the electron initially.

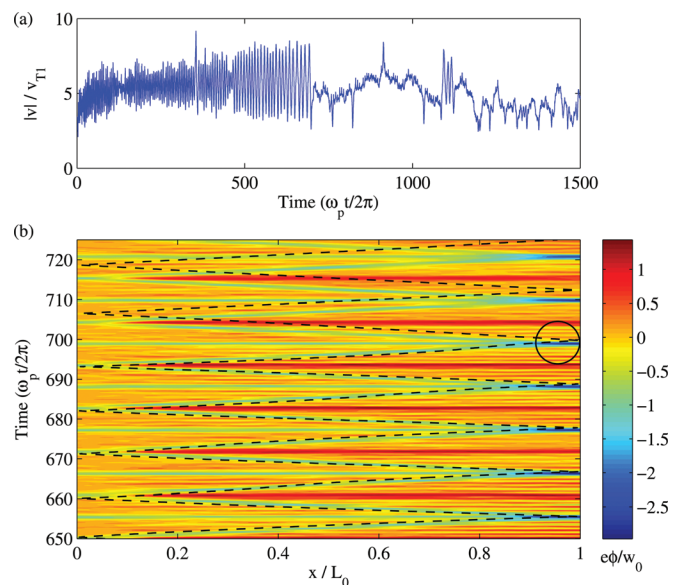


FIG. 3. (Color online) Electron detrapping from a nonlinear wave. (a) Electron absolute velocity $|v|$ normalized to v_{Ti} . (b) Coordinate of the electron, $x(t)/L_0$ (dashed; L_0 is the plasma initial length), superimposed on the potential energy $e\phi(x, t)$ measured in units of the particle average initial kinetic energy w_0 . The particle is trapped until $t \approx 700\tau_p$, at which point (circled) it escapes the potential well.

These results suggest that a BGK mode can be at an equilibrium in bounded plasma only as long as it does not reach the walls. On the other hand, one can see (Fig. 2) that dissipation caused by reflection is relatively weak, and nonlinear modes can persist on time scales far exceeding the transit time. Therefore, they represent robust structures, potentially applicable for mechanical manipulation through plasma compression, which will now be addressed.

III. AMPLIFICATION AND DAMPING THROUGH COMPRESSION

As shown in Refs. 4 and 5 for linear modes, the amplitude of an initially undamped Langmuir wave changes in time as plasma is compressed adiabatically. For example, it is seen from the conservation of the wave action $\mathcal{I} = W/\omega$, where W is the wave total energy, ω is the instantaneous frequency, $\omega = \omega_p(1 + 3k^2\lambda_D^2/2)$, k is the wavenumber, λ_D is the Debye length, and $\omega_p \propto V^{-1/2}$ is the electron plasma frequency, where the plasma volume V now varies in time. Thus, taking $W = W_0\omega/\omega_0$, with the subscript 0 henceforth denoting initial conditions, one obtains for the wave total electrostatic energy $W_E \propto \varepsilon^{-1/2}$ to lowest order in $\varepsilon \equiv L/L_0$. In other words, linear waves can be adiabatically amplified through compression, and what is shown below is that nonlinear waves can also be manipulated in a similar manner.

Figure 4 shows an example of the evolution of a solitary electron hole, same as in Fig. 1, as plasma is being compressed. (Note that the figure reads from right to left, with the system beginning at $\varepsilon = 1$ and compressing to a final state with $\varepsilon < 1$.) Like in simulations with linear waves,⁵ monotonic amplification is observed for the wave during most of the compression phase ($0.24 \lesssim \varepsilon < 1$). However, the amplitude is now amplified by a factor $G \approx 17$, much larger

than that reported in Ref. 5 for linear waves ($G < 2$), with G defined as the ratio of the peak electrostatic energy of the wave immediately prior to the onset of damping and the initial electrostatic energy of the wave prior to compression.

The amplification factor is increased for two reasons: (i) nonlinear modes do not experience Landau damping, and (ii) their amplitude changes more rapidly with ε . The latter, in turn, is due to the fact that the dynamics of a strongly nonlinear mode is determined primarily by phase-locked, resonant particles (cf. Ref. 19), unlike in a linear wave featuring few of those. Specifically, this is explained as follows.

First, notice that a localized electron hole has a characteristic length $\Delta < L$ [Fig. 1(f)]. Associated with that is a characteristic time scale during which reflection from a wall occurs, $T_r = \Delta/v_{ph} < T_{tr}$, where v_{ph} is the mode phase velocity. For parameters considered in this paper, T_r is a few times smaller than the characteristic bounce period τ_b ,²⁰ especially considering that most of trapped particles reside close to the separatrix. Hence, during the reflection time, the trapped particles are essentially free-streaming.

Second, notice that the distance D between two free-streaming particles with equal initial velocities is the same before and after reflection from a moving wall. This is because D is a Galilean invariant and obviously is conserved in the frame moving together with the wall. For $T_r \ll \tau_b$, the velocity spread over the trapping island is sufficiently small to guarantee also that the distance is conserved between *all* trapped particles. This means that the whole island also preserves its shape at reflection. Besides that, away from the walls, particles determining the nonlinear mode are phase-locked due to autoresonance. Therefore, the mode shape is not affected by moving walls, at least until it fits the system, i.e., as long as

$$\Delta/2 \lesssim L. \quad (2)$$

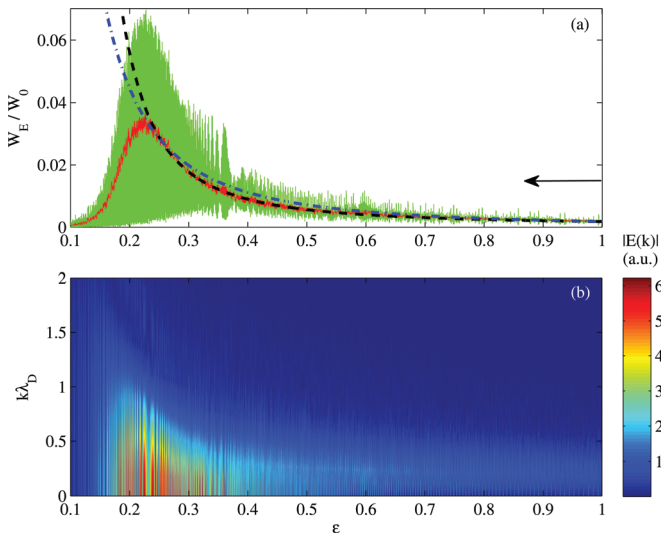


FIG. 4. (Color online) Evolution of a solitary electron hole during plasma compression. (a) Electrostatic energy W_E normalized to initial plasma total energy W_0 . Pictured are both the instantaneous and local time-averaged W_E (wide and thin line plots, respectively) and also the fitting functions $W_E/W_{E,0} = \exp[2.8(\varepsilon^{-1/2} - 1)]$ (dashed line) and $W_E/W_{E,0} = \varepsilon^{-2}$ (dashed-dotted line). (b) The absolute value of the electric field spatial Fourier spectrum $E(k)$ (in arbitrary units) vs compression parameter $\varepsilon = L(t)/L_0$ and wavenumber k , measured in inverse Debye lengths λ_D^{-1} , where $\lambda_D \propto \varepsilon^{-1/2}$. Note direction of time indicated by arrow in (a).

Conservation of the mode size under the condition (2) is indeed observed in simulations (Fig. 5) and allows one to predict the scaling for the electrostatic energy $W_E(\varepsilon)$ as follows. The electron density depletion due to the nonlinear mode results in an uncompensated background ion density δn_i . Since compression conserves the total number of particles, one has $\delta n_i \propto \varepsilon^{-1}$, assuming that, for simplicity, the electron hole total charge is also fixed. Hence, the characteristic field in the hole is $E \sim \delta n_i \Delta$, so conservation of Δ yields $W_E \propto \varepsilon^{-2}$. This estimate is, in fact, reasonably close to the scaling observed in simulations [Fig. 4(a)], although it was also found that the function $W_E/W_{E,0} = \exp[a(\varepsilon^{-1/2} - 1)]$, with $a = 2.8$, may be a somewhat better fit.

As also found in simulations (not shown here), a stable electron hole is produced if compression is halted while the condition (2) is satisfied. In the opposite case, though, the mode does not fit inside system, so outer orbits start to detrap. Rapid deterioration of the hole with further compression is then anticipated when the condition (2) is violated, and this is confirmed in simulations. For example, from Eq. (2), the mode in Figs. 4 and 5 is expected to persist until $\varepsilon \sim 0.2$, and this estimate is reasonably close to the value $\varepsilon \approx 0.24$ after which the rapid damping actually starts [Fig. 4(a)]. Remarkably, the subsequent wave evolution due to

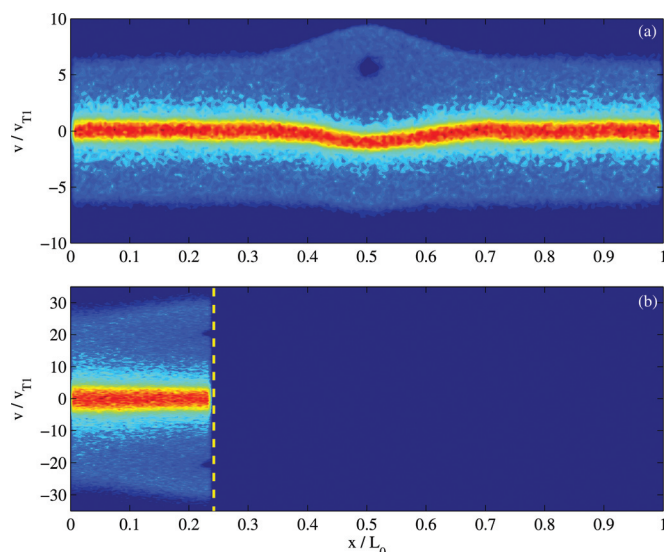


FIG. 5. (Color online) Phase space density snapshots (in arbitrary units, same color scale as Fig. 1) corresponding to the wave in Fig. 4. (a) Fully developed isolated electron hole at the beginning of compression, $\varepsilon = 1$. (b) The same hole at peak amplification immediately prior to onset of rapid damping, $\varepsilon = 0.24$. The outermost regions of the wave barely fit inside system, with the location of the moving wall marked by the dotted line, indicating that further compression will lead to detrapping of outer orbits.

collisionless damping is determined primarily by the instantaneous value of ε rather than the compression rate, as also confirmed in our simulations.

IV. DISCUSSION

By embedding waves in a plasma subject to compression, new tools for manipulating the plasma are made available. In the case of linear, initially undamped waves, it was found that some fraction of mechanical work exerted on the bulk plasma could be coupled into the coherent motion of the wave by means of the wave action conservation,⁴ and this wave energy could be sustained until a critical moment when a collisionless damping threshold was reached.⁵ Then, the localized wave energy could be channeled into the thermal energy of a particular species in a *switchlike* manner at a predetermined moment of time. Unlike heating the plasma at the start, embedding energy in the form of waves enables the concentration and confinement of energy in a form not subject to normal thermal diffusion. Furthermore, because nonlinear waves are already resonant with the thermal plasma, they are not subject to Landau damping, so that much higher compression ratios could be obtained before the onset of wave dissipation compared to the case involving initially undamped linear waves.⁵

There is also significant interest in generating and sustaining waves at high $k\lambda_D$, a goal that these resonant nonlinear waves are well-suited to accomplish. Even though k ceases to increase with compression, $k\lambda_D$ continues to increase, since thermal velocities grow faster than the plasma frequency. This means that, by means of compression, structures in the plasma are formed at high amplitude with an effectively high $k\lambda_D$.

Why is this important? There are several applications for insinuating high-amplitude high- $k\lambda_D$ structures in a plasma.

First of all, there is a possibility of using these structures effectively as a grating thereby to process laser light. This is particularly interesting in the regime where the light is intense enough to undergo compression effects through a nonlinear Raman decay process.²¹ The advantage of high- $k\lambda_D$ structures surviving near the plasma frequency is that lower-density plasma can then mediate the resonant decay between counterpropagating laser pulses. Absent the persistence of such structures, the phase-matching conditions would imply that the plasma wave at a low density has a lower phase velocity and therefore would be Landau-damped. The ability to use relatively lower-density plasma is particularly important in Raman compression for very short wavelength light, particularly for x-rays, where these surviving structures are absent, the higher densities needed would imply a smaller window in density-temperature space for which the compression effect survives.²²

In addition to using these structures to process light through wave-wave interactions, there may also be the possibility of manipulating particles through wave-particle interactions. The added flexibility of using these nonlinear structures at high amplitude facilitates a number of phase-space manipulations of particles with modes at phase velocities that would otherwise be unavailable at high amplitudes. This would be particularly important, for example, thereby to generate electric current and magnetic fields²³ or to channel energy to ions rather than to electrons.²⁴ (For the purposes of generating current, structures with only one sign of k would be employed, which means that the compression geometry would differ from the 1D compression examples considered here, where the walls are compressed in the direction of k ; rather, the compression or expansion would be perpendicular to k , but the principle would be the same.)

V. CONCLUSIONS

In this paper, the evolution of resonant, nonlinear Langmuir waves in a compressing plasma background was studied using PIC simulations. A major finding is that unlike linear waves, whose wavelength decreases proportionally to the system length, nonlinear waves, and in particular solitary electron holes, conserve their characteristic size during slow compression. This wavelength conservation leads to a substantially stronger adiabatic amplification of the wave as well as rapid collisionless damping when the wave no longer fits inside the system. If at any time the compression is halted, the resulting mode is stable and long-lived.

ACKNOWLEDGMENTS

The work was supported by the U.S. DOE under Contract No. DE-AC02-76-CH03073 and through the NNSA SSAA Program through DOE Research Grant No. DE-FG52-08NA28553.

¹E. I. Moses, *Nucl. Fusion* **49**, 104022 (2009).

²R. C. Kirkpatrick, I. R. Lindemuth, and M. S. Ward, *Fusion Technol.* **27**, 201 (1995).

³D. D. Ryutov, M. S. Derzon, and M. K. Matzen, *Rev. Mod. Phys.* **72**, 167 (2000).

- ⁴I. Y. Dodin, V. I. Geyko, and N. J. Fisch, *Phys. Plasmas* **16**, 112101 (2009); see also references therein.
- ⁵P. F. Schmit, I. Y. Dodin, and N. J. Fisch, *Phys. Rev. Lett.* **105**, 175003 (2010).
- ⁶P. F. Schmit, C. R. Mooney, I. Y. Dodin, and N. J. Fisch, *J. Plasma Phys.* (in press).
- ⁷K. Avinash, *Phys. Plasmas* **17**, 082105 (2010).
- ⁸I. Bernstein, J. M. Greene, and M. D. Kruskal, *Phys. Rev.* **108**, 546 (1957).
- ⁹M. M. Shoucri, *Phys. Fluids* **22**, 2038 (1979).
- ¹⁰H. L. Berk, C. E. Nielsen, and K. V. Roberts, *Phys. Fluids* **13**, 980 (1970).
- ¹¹H. L. Berk, B. N. Breizman, and N. V. Petviashvili, *Phys. Lett. A* **234**, 213 (1997); **238**, 408 (1998).
- ¹²T. H. Dupree, *Phys. Fluids* **25**, 277 (1982).
- ¹³K. Saeki, P. Michelsen, H. L. Pécseli, and J. J. Rasmussen, *Phys. Rev. Lett.* **42**, 501 (1979).
- ¹⁴L. Demeio and P. F. Zweifel, *Phys. Fluids B* **2**, 1252 (1990).
- ¹⁵H. Schamel, *Phys. Plasmas* **7**, 4831 (2000); see also references therein.
- ¹⁶A. Ghizzo, B. Izrar, P. Bertrand, E. Fijalkow, M. R. Felix, and M. Shoucri, *Phys. Fluids* **31**, 72 (1988).
- ¹⁷M. Buchanan and J. J. Dorning, *Phys. Rev. Lett.* **70**, 3732 (1993).
- ¹⁸L. Friedland, P. Khain, and A. G. Shagalov, *Phys. Rev. Lett.* **96**, 225001 (2006).
- ¹⁹V. B. Krapchev and A. K. Ram, *Phys. Rev. A* **22**, 1229 (1980).
- ²⁰R. W. B. Best, *Physica* **40**, 182 (1968).
- ²¹V. M. Malkin, G. Shvets, and N. J. Fisch, *Phys. Rev. Lett.* **82**, 4448 (1999).
- ²²V. M. Malkin, N. J. Fisch, and J. S. Wurtele, *Phys. Rev. E* **75**, 026404 (2007).
- ²³N. J. Fisch, *Rev. Mod. Phys.* **59**, 175 (1987).
- ²⁴N. J. Fisch and J. M. Rax, *Nucl. Fusion* **32**, 549 (1992); *Phys. Rev. Lett.* **69**, 612 (1992).